Supplementary Information

Bipolar ferrimagnetic semiconductor and doping concentration induced carrier spin flip in monolayer $NiMnBr_6$

Chenchen Lou,[a] Yujie Wang,[a] Chunlan Ma[a] and Jiayong Zhang*[a]

[a]Jiangsu Key Laboratory of Micro and Nano Heat Fluid Flow Technology and Energy Application, School of Physical Science and Technology, Suzhou University of Science and Technology, Suzhou, 215009, China

*Corresponding author: jyzhang@usts.edu.cn

Supporting Note 1

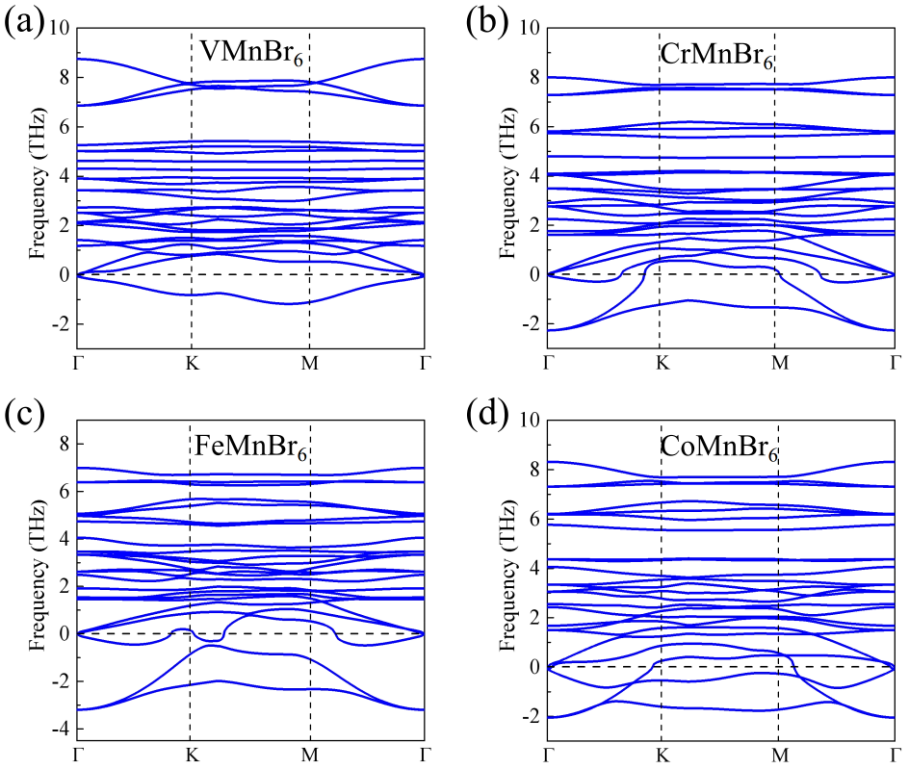

Fig. S1 (a-d) The calculated phonon spectra for the monolayer $VMnBr_6$ (a), monolayer $CrMnBr_6$ (b), monolayer $FeMnBr_6$ (c), monolayer $CoMnBr_6$ (d).

Supporting Note 2

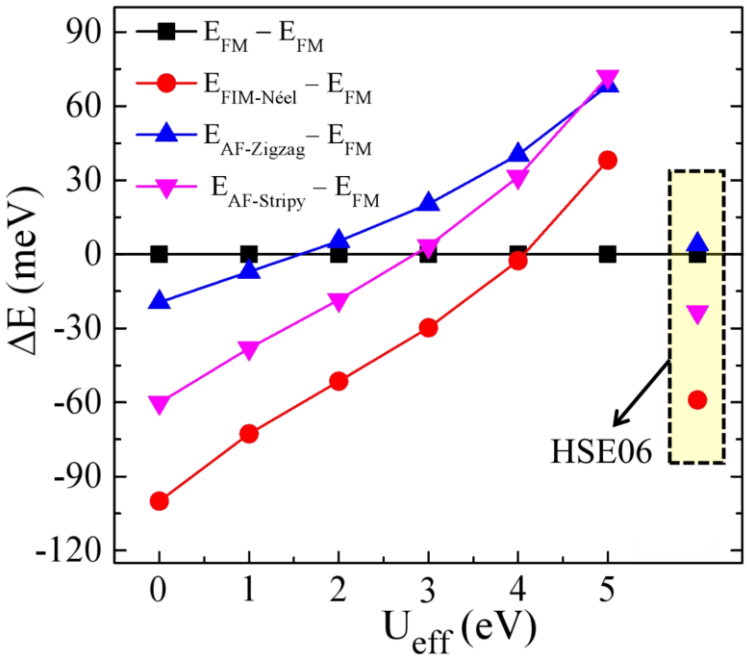

Fig. S2 The energy differences (ΔE) between FM and FM state ($E_{\mathrm{FM}} - E_{\mathrm{FM}}$), FIM-Néel and FM state ($E_{\mathrm{FIM-Néel}} - E_{\mathrm{FM}}$), AF-Zigzag and FM state ($E_{\mathrm{AF-Zigzag}} - E_{\mathrm{FM}}$), and AF-Stripy and FM state ($E_{\mathrm{AF-stripy}} - E_{\mathrm{FM}}$) as a function of effective Hubbard U_{eff} (U_{eff} = U − J) for the monolayer $NiMnBr_6$. The energy differences (ΔE) obtained by using the HSE06 calculations are given in the dotted bordered rectangle.

Supporting Note 3

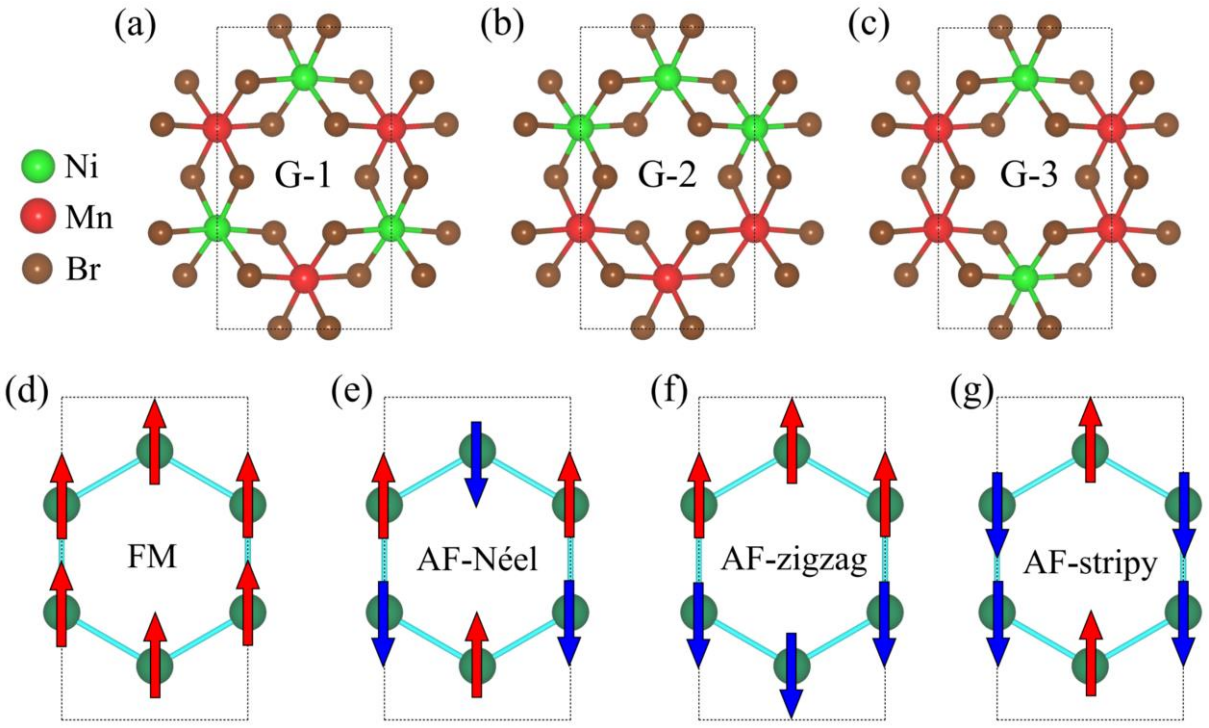

Fig. S3 (a-c) The three possible distributions of the Mn atoms replacement with Ni atoms in a monolayer $NiMnBr_6$ rectangular supercell: G-1 (a), G-2 (b), and G-3 (c). (d-g) The four different magnetic configurations considered for the monolayer $NiMnBr_6$ rectangular supercell: FM (d), AF-Néel (e), AF-zigzag (f), and AF-stripy (g). Up and down spins are denoted by the red up and blue down arrows, respectively.

Table SI The calculated total energies of the monolayer $NiMnBr_6$ rectangular supercell ($Ni_2Mn_2Br_{12}$) in G-1, G-2, and G-3 atomic structures with the FM, AF-Néel, AF-zigzag, and AF-stripy magnetic configurations.

$Ni_2Mn_2Br_{12}$	FM (eV)	AF-Neel (eV)	AF-zigzag (eV)	AF-stripy (eV)
G-1	-51.939409	-51.990853	-51.934098	-51.957870
G-2	-51.776044	-51.661059	-51.755106	-51.680767
G-3	-51.771654	-51.710440	-51.723194	-51.768831

Supporting Note 4

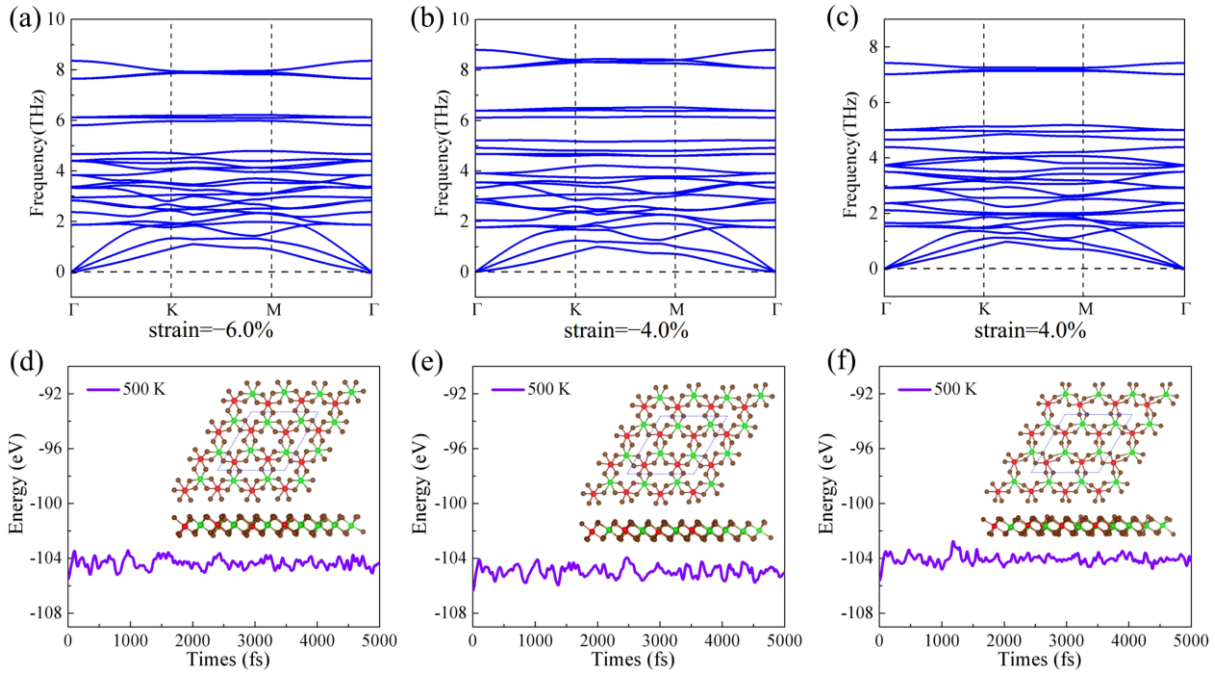

Fig. S4 (a-c) The calculated phonon spectra for the strain=−6.0% (a), strain=−4.0% (b), and strain=4.0% (c) monolayer $NiMnBr_6$. (d-f) The fluctuation of total energies of the strain=−6.0% (d), strain=−4.0% (e), and strain=4.0% (f) monolayer $NiMnBr_6$ system with respect to time during AIMD simulations at 500 K. The insets in (d-f) show the top and side views of atomic configuration snapshots from AIMD simulations after 5.0 ps.

Supporting Note 5

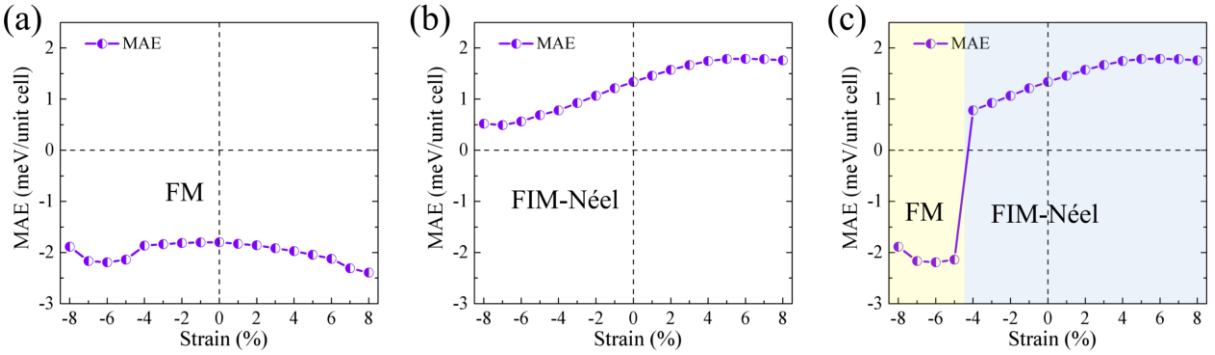

Fig. S5 (a) The calculated MAEs with respect to strain (−8.0% to 8.0%) for monolayer $NiMnBr_6$ with the FM magnetic configuration. (b) The calculated MAEs with respect to strain (−8.0% to 8.0%) for monolayer $NiMnBr_6$ with the FIM-Néel magnetic configuration. (c) The calculated MAEs with respect to strain (−8.0% to 8.0%) for monolayer $NiMnBr_6$ with magnetic ground state.

Supporting Note 6

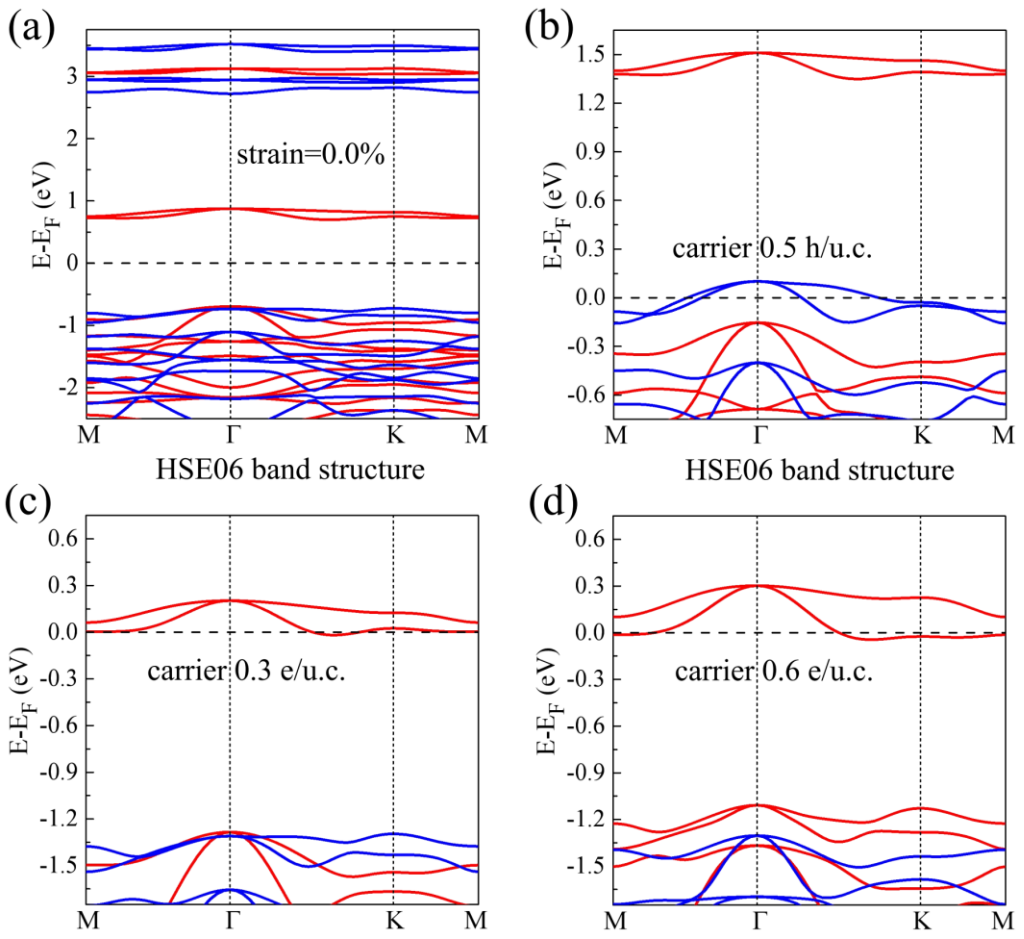

Fig. S6 (a) The spin-polarized band structure of the 0.0% strained (strain=0.0%) monolayer $NiMnBr_6$. (b-d) The spin-polarized band structures of the strain=0.0% monolayer $NiMnBr_6$ with carrier doping concentration of 0.5 hole (b), 0.3 electron (c), and 0.6 electron (d) per unit cell. The red and blue curves denote the spin-up and spin-down bands, respectively. All the band structures are calculated by using the HSE06 functional.

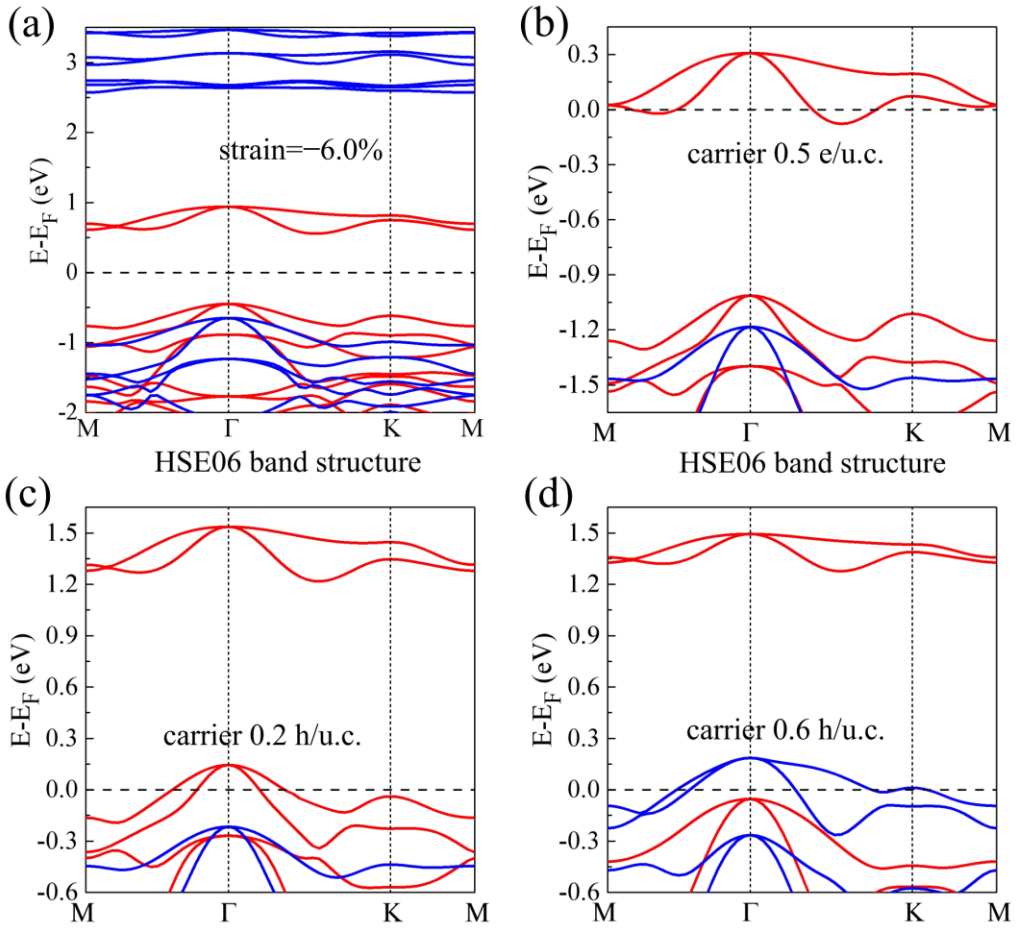

Fig. S7 (a) The spin-polarized band structure of the 6.0% compressive strained (strain=−6.0%) monolayer $NiMnBr_6$. (b-d) The spin-polarized band structures of the strain=−6.0% monolayer $NiMnBr_6$ with carrier doping concentration of 0.5 electron (b), 0.2 hole (c), and 0.6 hole (d) per unit cell. The red and blue curves denote the spin-up and spin-down bands, respectively. All the band structures are calculated by using the HSE06 functional.